Kumjian, M. R., 2011: Precipitation properties of supercell hook echoes. *Electronic J. Severe Storms Meteor.*, **6** (5), 1–21.

Electronic Journal of
SEVERE STORMS METEOROLOGY

Precipitation Properties of Supercell Hook Echoes

MATTHEW R. KUMJIAN
Cooperative Institute for Mesoscale Meteorological Studies,
Atmospheric Radar Research Center, University of Oklahoma, and
NOAA/OAR/National Severe Storms Laboratory, Norman, Oklahoma

(Submitted 28 April 2011; in final form 5 October 2011)

ABSTRACT

Recent studies have suggested that thermodynamic properties of supercell rear-flank downdrafts (RFDs) can affect whether or not tornadogenesis occurs. The thermodynamic characteristics of RFDs are determined in part by microphysical processes such as evaporation of raindrops and melting of hailstones. Whereas in situ measurements of hook-echo particle size distributions (PSDs) are exceedingly rare, polarimetric radars can be used to determine the bulk characteristics of these PSDs remotely. A preliminary analysis of polarimetric radar data from a small sample of supercell hook echoes reveals unusual drop size distributions compared to typical rainfall in Oklahoma, as well as spatially inhomogeneous structures. The inner edge of the hook echo is often characterized by low or moderate reflectivity factor at horizontal polarization (Z_H), with very high differential reflectivity factor (Z_{DR}), indicating a sparse population of very large drops. The southern and/or western (back) portion of the hook is characterized by moderate to high Z_H and rather low Z_{DR}, indicating a surplus of small drops and/or a lack of larger drops. Hypotheses explaining the unusual drop size distributions are presented. Additionally, the time evolution of these characteristics is explored using data collected with a special rapid scanning strategy.

1. Introduction

According to recent research, tornadogenesis can be affected by the thermodynamic properties of supercell rear-flank downdrafts (RFDs). Observational studies by Markowski et al. (2002) and Grzych et al. (2007) demonstrate that supercells which produced significant (F2+ rated) tornadoes had RFDs with smaller deficits of both θ_e and virtual potential temperature than the RFDs of weakly tornadic or nontornadic supercells. Idealized numerical simulations by Markowski et al. (2003) support these findings, suggesting that excessively cold RFDs are associated with relatively weak surface convergence that cannot stretch vertical vorticity to tornadic magnitudes.

Corresponding author address: Matthew Kumjian, 120 David L. Boren Blvd., National Weather Center 4900C, Norman, OK 73071, E-mail: matthew.kumjian@noaa.gov

Exceptions have been found, however, where tornadoes were present in more negatively buoyant RFDs (e.g., Hirth et al. 2008; Romine et al. 2008). Thus, while not telling the whole story, thermodynamic properties of the RFDs are seemingly important for storm dynamics and evolution (Markowski et al. 2002).

The thermodynamic characteristics of RFDs are determined in part by microphysical processes such as evaporation of raindrops and melting of hailstones. The thermodynamic characteristics and microphysical processes both contribute to changes in the particle-size distributions within the hook echo. To date, the precipitation properties of supercell hook echoes are unknown, with only a small amount of data collected (e.g., Schuur et al. 2001; Dawson and Romine 2010). In addition, the spatial distribution of the bulk precipitation characteristics within hook echoes is not known. Whereas in situ measurements of the spatial or temporal changes in the hook echo particle size

distributions (PSDs) are exceedingly rare, dual-polarization radars can be used to determine the bulk PSD characteristics remotely. Such polarimetric radar observations made in Oklahoma at S and C bands are presented in this study and reveal raindrop size distributions (DSDs) in hook echoes atypical of those expected in Oklahoma rainfall. These observations are presented in the following section, along with a primer on the interpretation of polarimetric radar variables. Section 3 provides a discussion on possible explanations of the unusual PSDs. In section 4, data from a special rapid-scan case are presented, allowing a unique look at the evolution of the precipitation characteristics of a hook echo throughout the occlusion of the low-level mesocyclone. Section 5 summarizes the conclusions and offers a conceptual model of the proposed phenomena.

2. Observations

a. Overview of the polarimetric variables

The polarimetric radar variables are described briefly here with an emphasis on physical interpretation. The reader is referred to other sources for more in-depth descriptions of the available measurements from dual-polarization radars (Herzegh and Jameson 1992; Doviak and Zrnić 1993; Zrnić and Ryzhkov 1999; Straka et al. 2000; Bringi and Chandrasekar 2001; Ryzhkov et al. 2005a).

The differential reflectivity factor (Z_{DR}) is the logarithm of the ratio of backscattered power at horizontal and vertical polarizations and is dependent on hydrometeor shape, size, orientation, density, and water content. However, it is independent of particle concentration. Raindrop oblateness increases with diameter (e.g. Pruppacher and Beard 1970), and Z_{DR} increases with increasing raindrop oblateness, so Z_{DR} in rain can be considered as a measure of median drop size within the radar sampling volume. In typical rainfall, Z_{DR} increases with increasing reflectivity factor at horizontal polarization (Z_H), owing to the higher concentration of larger drops in heavier rain. For spherical particles or those with isotropic scattering properties (e.g., a chaotically tumbling hailstone), Z_{DR} is 0 dB. For hydrometeors of a given shape and size, Z_{DR} increases with higher density and/or liquid water content. Therefore, regions of the storm with observed high Z_{DR} are mostly associated with large, wet hydrometeors.

Because of raindrop oblateness, the forward-propagating transmitted radar wave will accumulate a phase difference between its horizontally-polarized and vertically-polarized components as it passes through precipitation. This phase difference is known as the differential propagation phase shift (Φ_{DP}), and arises from the fact that the horizontally-polarized wave encounters "more" of a given raindrop than does the vertically-polarized wave, causing it to lag behind the vertically-polarized wave. Though Φ_{DP} generally increases monotonically with range in rain, differential phase shifts upon backscattering (δ) that arise from resonance scattering are superposed on the signal and can cause positive or negative departures from this monotonicity. Often, it is convenient to compute the range derivative of Φ_{DP}, known as the specific differential phase (K_{DP}). Owing to its dependence on hydrometeor concentration, K_{DP} offers similar information to that obtained from Z_H, though K_{DP} is not affected by heavily aggregated snow or dry graupel/hail and has a weaker dependence on particle diameter D ($K_{DP} \sim D^{4.24}$; $Z_H \sim D^6$).

The co-polar cross-correlation coefficient (ρ_{hv}) is a measure of diversity of scatterers within the radar sampling volume. Whereas it is near unity in pure rain (>0.98 at S band) or pure dry hail, a mixture of particle types within the sampling volume will decrease ρ_{hv} values. Additionally, diversity of particle sizes (if nonspherical), orientations, shapes, and dielectric constants within the sampling volume will decrease the ρ_{hv}. Variations of δ within a radar volume will substantially reduce ρ_{hv}; therefore, the measured ρ_{hv} is significantly reduced in the presence of resonance (Mie) scatterers. Note that at C band, large raindrops (equivolume diameters of about 5–6 mm) are resonance scatterers, so their presence in a sampling volume can reduce ρ_{hv} as low as ~0.93 in pure rain.

b. Methods

The data presented in this section were collected by the polarimetric prototype WSR-88D radar in Norman, OK (KOUN), and the University of Oklahoma Polarimetric Radar for Innovations in Meteorology and Engineering (OU-PRIME; Palmer et al. 2011). KOUN data were corrected for both attenuation and differential attenuation, calibrated, and processed

following Ryzhkov et al. (2005a). Similarly, OU-PRIME data were processed as described in Palmer et al. (2011). Only data from low-level scans were considered. The particular scans were chosen to: 1) minimize ground clutter contamination and biases from partial beam blockage, and 2) obtain data from less than ~1 km AGL. The location of the hook echo was determined subjectively from investigating plan position indicators (PPIs) of Z_H. For each of the cases shown, the hook echo was well-defined and displayed a classic cyclonically curved shape. Radar range gates within the subjectively defined hook echo were selected manually and consisted of the entire appendage up to where it joined the main body of the storm (i.e., the main precipitation echo). Data points from KOUN included in the quantitative analysis below were subjected to a stringent ρ_{hv} threshold of ≥0.98, in order to retain rain points but to discard points associated with nonmeteorological scatterers (e.g., tornadic debris, light debris along the RFD gust front, etc.) as well as those radar sampling volumes containing a mixture of rain and hail. Note that such a threshold cannot be applied to the C-band (OU-PRIME) cases because the ρ_{hv} in heavy rain at C band heavily overlaps values found in the rain/hail mixture (e.g., ρ_{hv} can be as low as ~0.93 in pure rain at C band).

c. Data

Data from six supercell storms are presented in this analysis (Table 1), four of which were observed by KOUN, and two by OU-PRIME. Low-level PPIs of Z_H from each KOUN case are shown in Fig. 1. Each of the KOUN cases was analyzed as described above. Figure 2 is a series of Z_H–Z_{DR} scattergrams from these four KOUN cases shown in Fig. 1. Overlaid on each scattergram is the Cao et al. (2008) Z_H–Z_{DR} relation:

$$Z_{DR} = 10^{\left(-2.6857\cdot10^{-4} Z_H^2 + 0.04892 Z_H - 1.4287\right)}, \quad (1)$$

where both Z_H and Z_{DR} are expressed in logarithmic scale. Equation (1) was derived from numerous DSDs in Oklahoma rainfall and serves as an indication of what is "expected" in typical rainfall events (both stratiform and convective). The data reveal similarities between the hook echo precipitation characteristics in each case. Notably, each storm's hook echo produces data points for Z_H above about 40–45 dB*Z* that have Z_{DR} values below what is expected in Oklahoma rainfall, as indicated by the Cao et al. (2008) relation. In Fig. 1c, there is a particularly striking separation between these hook echo points (red asterisks) and points from the rest of the storm (black dots). Such Z_H–Z_{DR} pairs beneath the Cao et al. curve indicate particle size distributions with more spherical scatterers than is typical in Oklahoma rainfall. The high ρ_{hv} values used in the analysis strongly suggest that the radar resolution volumes were sampling pure rainfall. Thus, some of the measurements in hook echoes reveal DSDs with larger-than-expected concentrations of smaller drops and a relative lack of larger drops. Each case also produces hook echo points with large (>3 dB) Z_{DR} for Z_H <30 dBZ, which indicates large drops in the sampling volumes. Such "large drop" points for lower Z_H values indicate a DSD skewed towards a sparse concentration of large drops and a relative deficit of small drops.

Table 1: List of cases included in the analysis, including the date, time, and observing radar (OU' means OU-PRIME).

Date	Time (UTC)	Radar
10 May 2003	0345	KOUN
30 May 2004	0044	KOUN
31 March 2008	0325	KOUN
1 June 2008	0331–0351	KOUN
10 May 2010a (Moore)	2231	OU'
10 May 2010b (Norman)	2242	OU'

Notice also the tendency for points from the rest of the storm (black dots) to lie above the Cao et al. (2008) curve for all values of Z_H, indicating larger-than-expected Z_{DR} values. In convective storms (especially supercells), hail production can be prolific, leading to large quantities of small hailstones. Smaller hailstones (diameters ~6–15 mm) all melt to produce large drops 6–8 mm in diameter, leading to an enhancement of the concentration of "big drops" (Ryzhkov et al. 2009). This amplifies the observed Z_{DR} signal, regardless of the number of small drops present in the distribution. Thus, Z_{DR} is higher than "expected" from the Cao et al. (2008) relation for most values of Z_H in the supercells presented herein. The data points with high Z_{DR} and lower Z_H imply a distribution strongly skewed to large drops with a relative deficit of smaller drops; these smaller drops tend to contribute to increased Z_H.

The data reveal unusual DSDs in hook echoes, but also suggest large variability (i.e., a wide scatter). Conventional presentation of the data in PPIs provides insight into the spatial distribution and heterogeneities of precipitation characteristics in hook echoes, albeit in a less quantitative manner.

Low-level scans during a long-track F4 tornado that struck Moore, OK on 10 May 2003 (Fig. 3) reveal complex patterns in the polarimetric variables. At the radar-relative location of the tornado (x = 7 km, y = 39 km), a tornadic debris signature is evident as high Z_H, low Z_{DR}, and very low ρ_{hv} (Ryzhkov et al. 2005b). A Z_{DR} arc (Kumjian and Ryzhkov 2008, 2009) is present along the southern edge of the forward-flank echo (Fig. 3b). High Z_{DR} values are seen wrapping around the western side of the tornado, along the inner (inflow) edge of the Z_H hook echo. Behind the high-Z_{DR} values, at the back of the hook echo and wrapping around the southern and southeastern sides of the tornado, are regions of 45–55 dBZ with Z_{DR} <1.5 dB (and <1 dB in some places). This region is also marked by high K_{DP}, indicating large liquid water content, and very high ρ_{hv}, indicating low diversity among hydrometeors and likely signifying pure rain. Thus, the polarimetric variables indicate distinct regions of large drops (in the Z_{DR} arc and extending around the inside edge of the hook echo) and smaller drops (in the back of hook echo and to the south and southeast of the tornado).

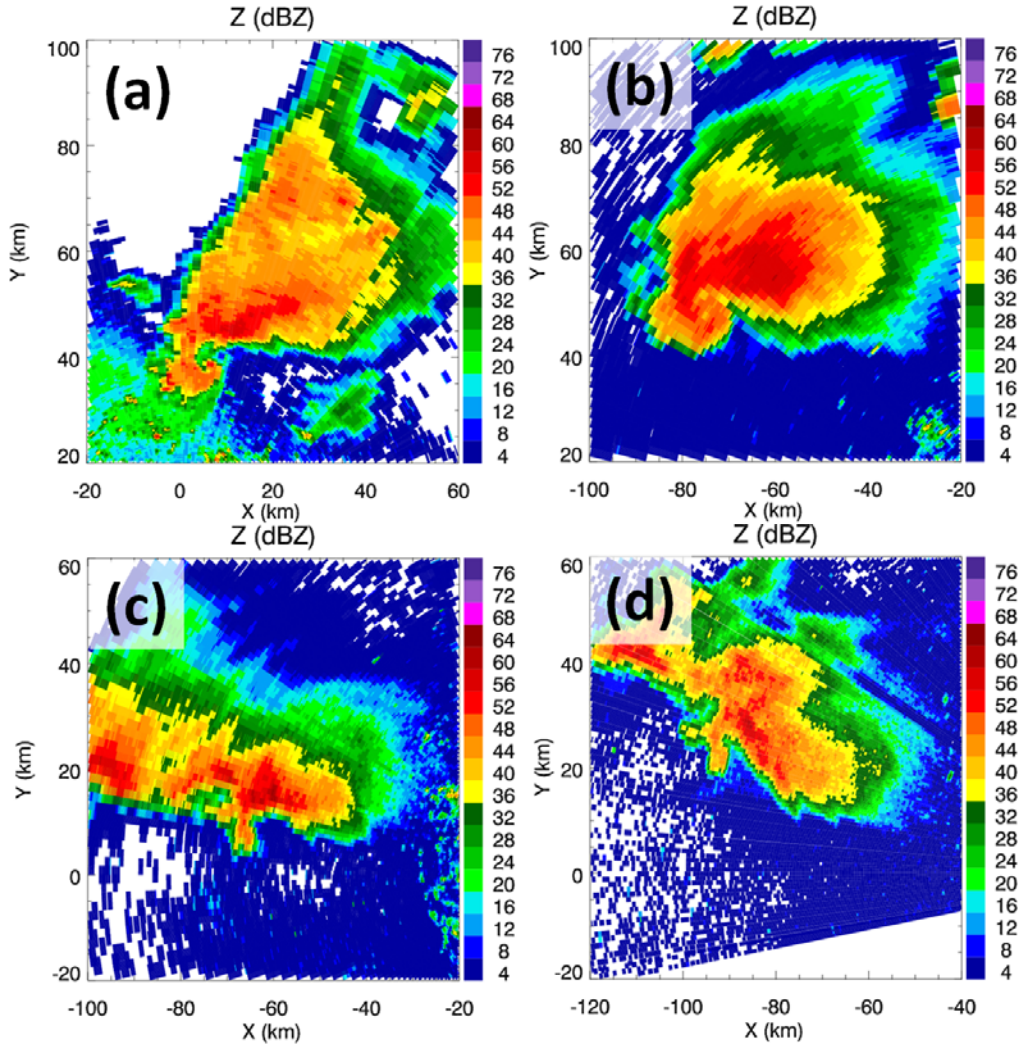

Figure 1: Low-level PPIs of Z_H measured by KOUN for the first four cases in Table 1. Data are from: a) 0345 UTC 10 May 2003, b) 0044 UTC 30 May 2004, c) 0325 UTC 31 March 2008, and d) 0340 UTC 1 June 2008. *Click image to enlarge.*

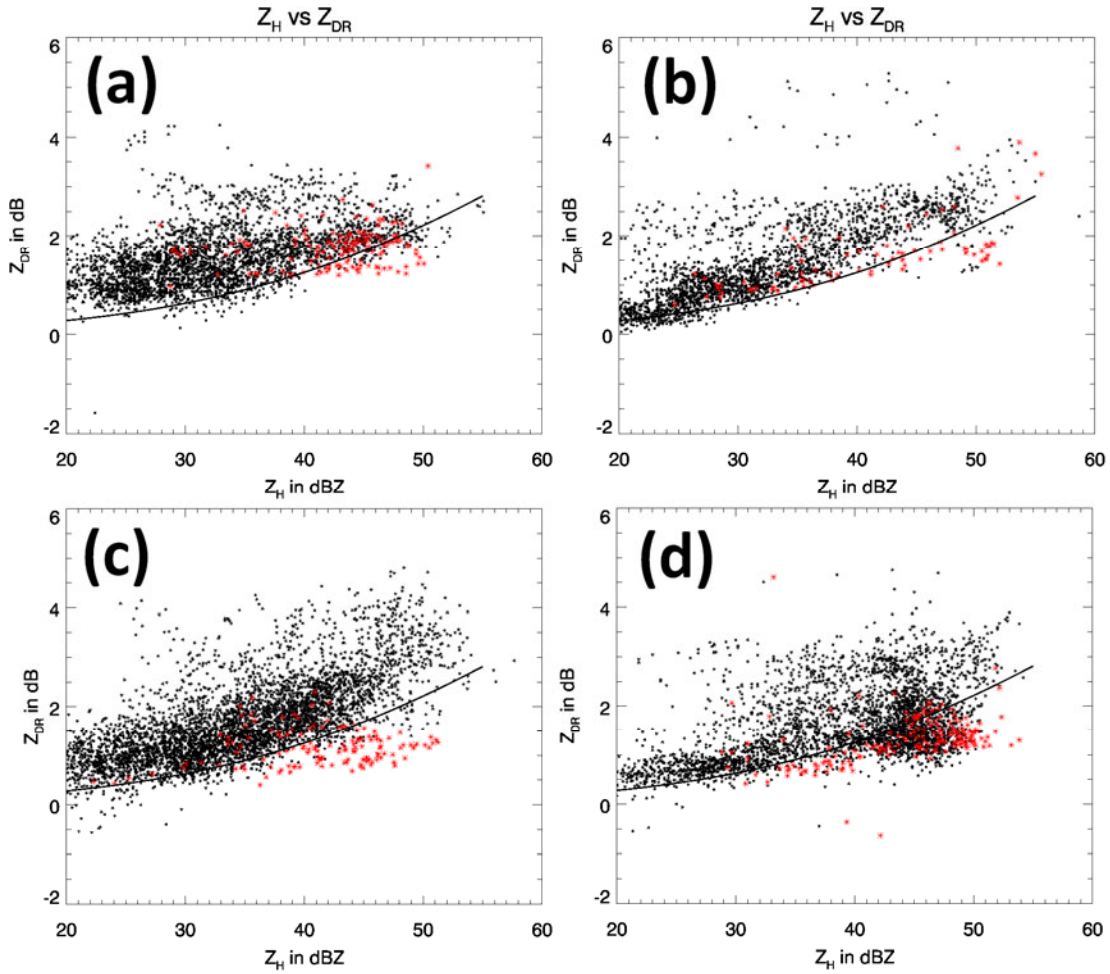

Figure 2: Scattergrams of Z_H and Z_{DR} from the four KOUN supercell cases: a) 0044 UTC 29 May 2004, b) 0325 UTC 31 March 2008, c) 0340 UTC 1 June 2008, and d) 0345 UTC 10 May 2003. Black points represent data from the entire low-level scan of the storm; whereas red points are from the hook echo. Data have been thresholded with $\rho_{hv} \geq 0.98$ to prevent contamination from the tornadic debris signature and to ensure the points are mainly from raindrops. Overlaid on each panel is the Cao et al. (2008) relation indicating the expected Z_{DR} for a given Z_H in Oklahoma rainfall. *Click image to enlarge.*

A similar pattern is observed in other cases, including another EF4 tornado in Moore, OK on 10 May, this time in 2010 (Fig. 4). Data were collected contemporaneously by the S-band KOUN and the C-band OU-PRIME. At C band, large raindrops enhance positive Z_{DR} signatures because of resonant scattering effects; therefore, spatial gradients of median drop sizes result in more pronounced gradients of Z_{DR} at C band than at S band. Similarly, ρ_{hv} can be lower at C band, even in pure rain, owing to Mie scattering effects (if drops with diameters between ~5–6 mm are present). In Fig. 4a, the tornado is at the center of the image, surrounded by bands of enhanced Z_H. In Fig. 4b, higher Z_{DR} is observed wrapping about three quarters of the way around the tornado, which itself is evident in the pronounced tornadic debris signature, especially in ρ_{hv} (Fig. 4d). On the southeastern quadrant of the circulation, however, a pocket of lower Z_{DR} (0–2 dB) is seen wrapping cyclonically around the tornado, as indicated by the curved arrow. This small-drop region is characterized by Z_H values between 35–45 dB*Z*, modest Φ_{DP} (<10°), and very high (>0.975) ρ_{hv}.

About 11 min later, another supercell produced a destructive tornado (eventual EF4) that developed just 200 m south of the National Weather Center, in Norman, OK. The extremely close proximity to OU-PRIME afforded a unique view of the storm, especially the hook echo and

tornado (Fig. 5) that were captured with very high spatial resolution (Palmer et al. 2011; Bodine et al. 2010). The hook echo from this particular storm is extremely thin, <1 km wide at its narrowest point (Fig. 5a). At the tip of the hook echo, a debris "ball" of high Z_H, low Z_{DR}, and very low ρ_{hv} is observed. Even the "eye" of the tornado is apparent, likely due to a combination of centrifuging of debris (e.g., Dowell et al. 2005) and subsidence in the core of the vortex (e.g., Wurman and Gill 2000). Along the hook echo, a striking gradient in Z_{DR} and ρ_{hv} is evident (Fig. 5b,c), with very large drops located along the inner edge of the hook, with considerably smaller drops along the back edge (and extending farther north to the rear of the storm). Though Z_{DR} is low to the south and southeast of the tornado, as in the other cases, the ρ_{hv} is also considerably lower than expected in pure rain. It is likely that light debris was lofted by the strong RFD winds, as blowing dust was visible from the National Weather Center. Similar features are observed with KOUN at this time (not shown).

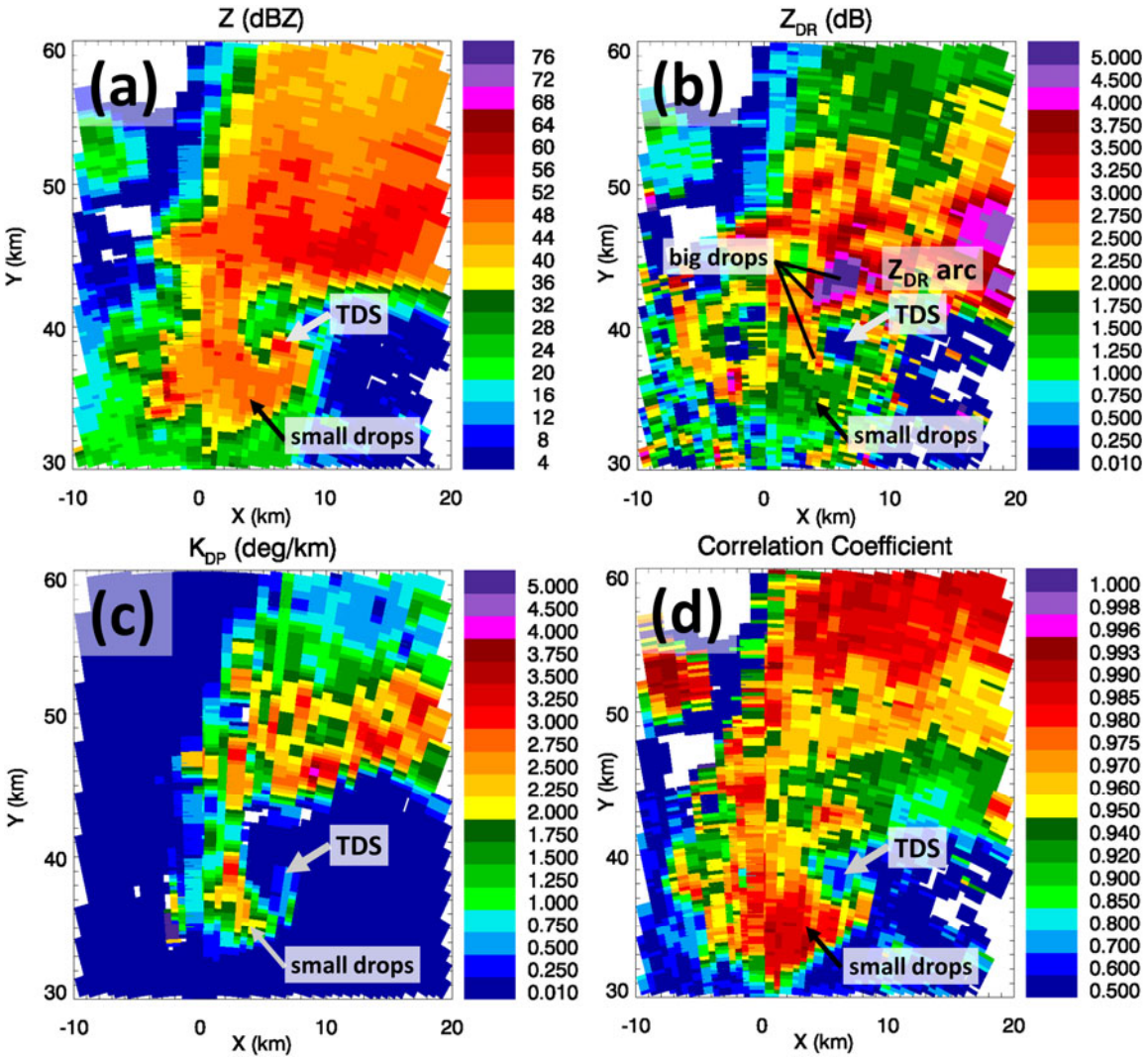

Figure 3: Low-level PPI scan from KOUN, 0345 UTC 10 May 2003, during a long-track damaging tornado (located at x = 7 km, y = 39 km). Fields of variables shown are: a) Z_H, b) Z_{DR}, c) K_{DP}, and d) ρ_{hv}. Visible are the tornadic debris signature (TDS), the disrupted Z_{DR} arc, a region of large drops wrapping around the inside of the hook echo, and a region of small drops to the southwest and south of the tornado. *Click image to enlarge.*

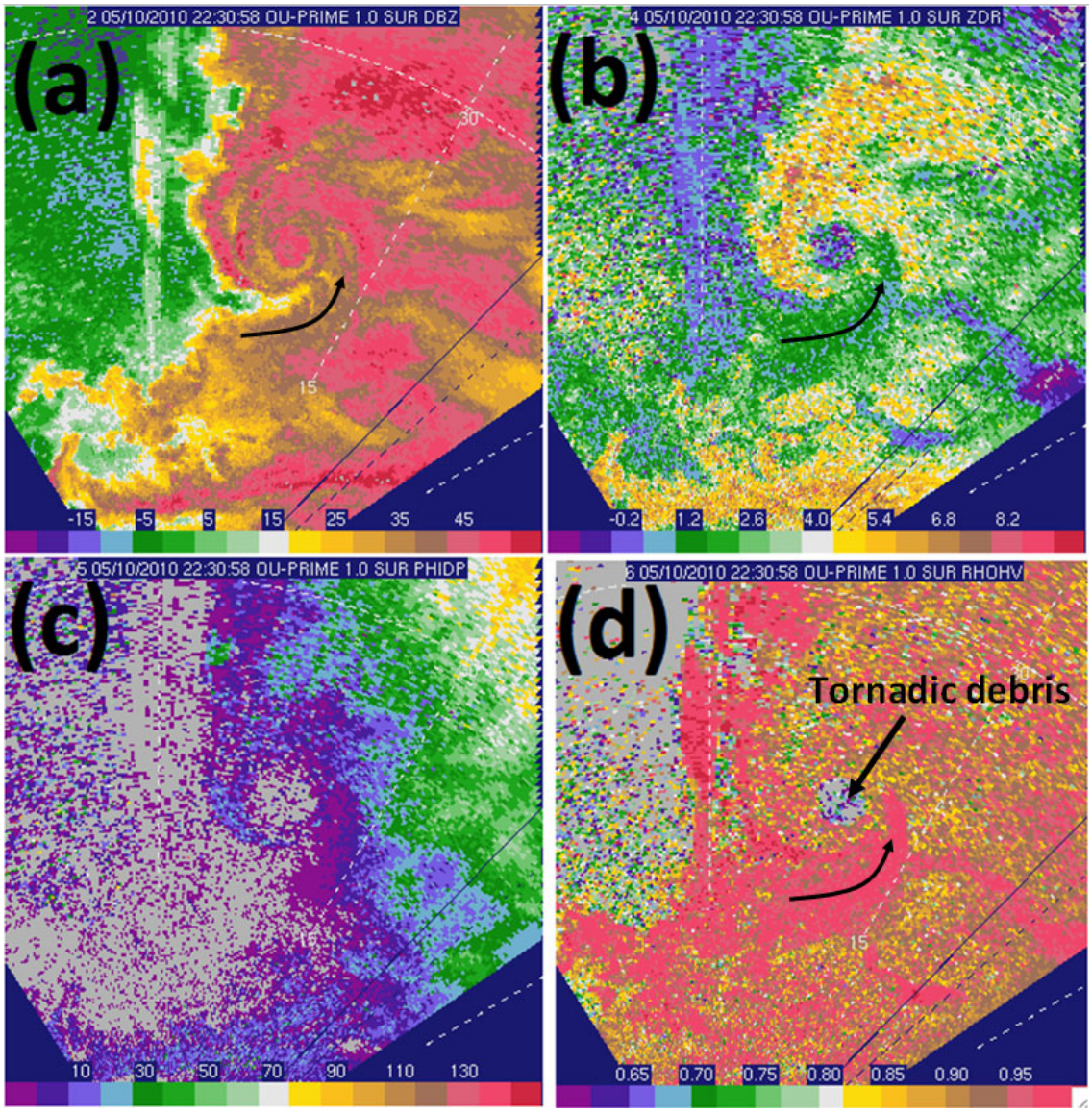

Figure 4: Observed fields of a) Z_H, b) Z_{DR}, c) Φ_{DP}, and d) ρ_{hv} from 2231 UTC 10 May 2010. Data from the C-band OU-PRIME at 1.0° elevation (beam height at the location of the tornado is ≈400 m AGL). Dotted radial isopleths are plotted every 30° in azimuth, with 15-km and 30-km ranges indicated on the 30° isopleth. The 30-km range ring is also plotted. *Click image to enlarge*

3. Discussion and explanation

The preceding analysis suggests that a common feature of polarimetric radar observations of supercell hook echoes (at least in the 6 cases presented herein) is a region of high Z_{DR} along the inflow edge of the Z_H gradient, sometimes connecting with the Z_{DR} arc. On the back side of the hook, and wrapping around to the south and southeast of the tornado (if one is present) is a region of considerably smaller Z_{DR}. The overall distribution of Z_H–Z_{DR} is markedly different from typical Oklahoma rainfall.

Though a given Z_H–Z_{DR} data point in a hook echo is possible in other precipitation systems, the collective dataset demonstrates the atypical nature of hook echo DSDs (Fig. 6). The large cluster of points with Z_H values between about 40–50 dBZ for Z_{DR} values less than ~1.0–1.5 dB is unusual for a precipitating system in Oklahoma, and better matches what is expected in tropical rain (e.g., Cao et al. 2008).

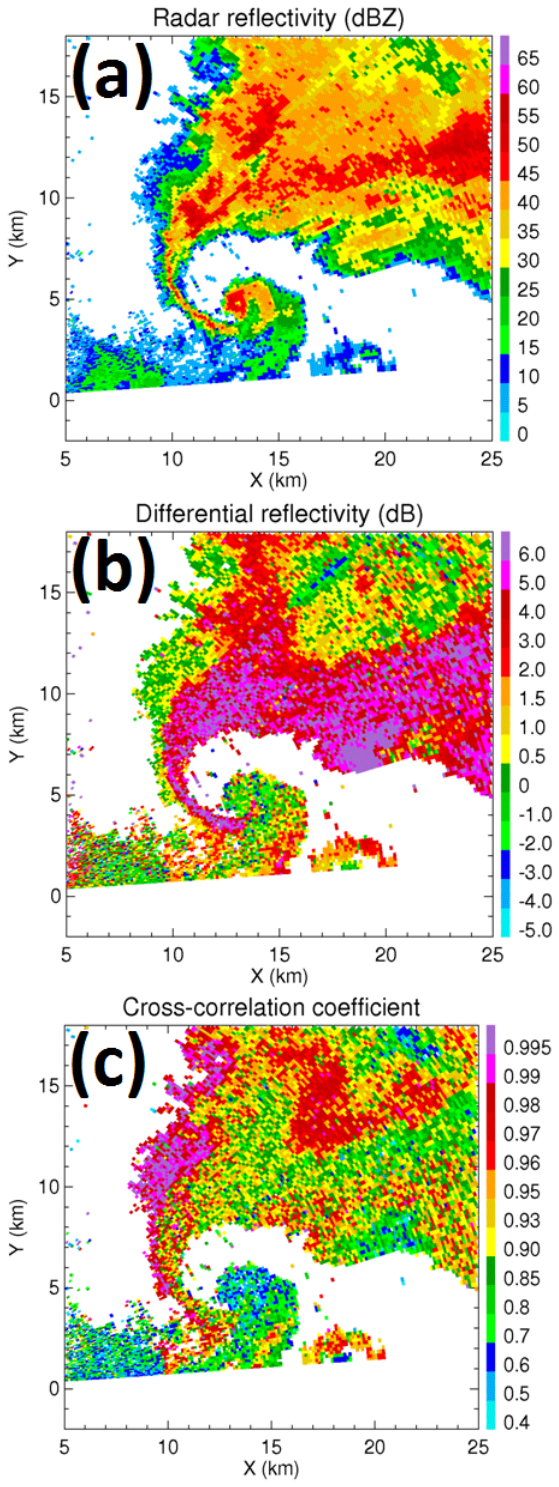

Figure 5: Observed fields of a) Z_H, b) Z_{DR}, and c) ρ_{hv}, 2242 UTC 10 May 2010, from the C-band OU-PRIME. The main tornado is located at about x = 13 km, y = 5 km. Another tornado is partly cut off by the sector, located at about x = 18.5, y = 1.5 km. *Click image to enlarge.*

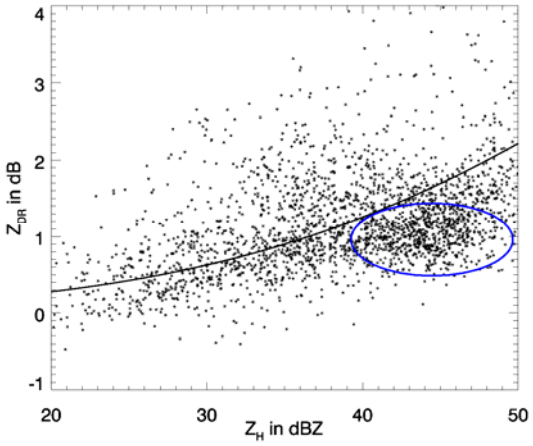

Figure 6: Z_H–Z_{DR} points from the hook echo of the 1 June 2008 supercell, observed at low levels (<1 km AGL). Data are from 0331–0351 UTC and are subject to a threshold $\rho_{hv} \geq 0.97$. Overlaid is the Cao et al. (2008) curve for typical rainfall in Oklahoma. The dense cluster of points between 40–50 dB*Z*, beneath the Cao et al. curve, indicates unusual DSDs compared to typical Oklahoma rainfall (highlighted by the blue ellipse). *Click image to enlarge*

The consistent localization of regions of small and large drops in hook echoes, inferred from the small sample of polarimetric radar data PPIs presented above, suggests similar mechanisms at work in each case, such as a microphysical or dynamic process intrinsic to supercells. But are these processes unique to supercells? One approach to this question is to assess the DSDs themselves; in other words, how similar or dissimilar are DSDs in supercell hook echoes to DSDs in other precipitating systems?

At the time of this writing, the only published study to observe the DSD in a supercell RFD using a disdrometer is from Schuur et al. (2001), who state that the observed DSD in the RFD "had a much larger small drop [<1 mm in diameter] concentration than was measured for any of the previous three cases" they investigated, which included weak convective rainbands, widespread stratiform rain, and a mesoscale convective system. More such measurements are needed. Encouragingly, preliminary results from VORTEX2 disdrometer measurements (e.g., Dawson and Romine 2010) also reveal exotic DSDs in and around the supercell RFD, including one with a large concentration of small drops and a total lack of larger drops

(their Fig. 4). In fact, the DSD sampled in the rear of the hook echo did not contain appreciable concentrations of drops >1.5 mm in diameter. Though such observations are limited, they provide some evidence in support of inferences made from dual-polarization radar measurements that DSDs in hook echoes are atypical of those encountered in ordinary Oklahoma rainfall. This suggests that processes distinctive to supercell storms or their environments may contribute to the production of exotic DSDs in the hook echo. Hypotheses describing plausible explanations for these exotic DSDs are presented in the next subsections. These hypotheses are rooted in the existing body of work on supercell microphysics and dynamics. Through eliminating the explanations with weaker standing, we arrive at what we consider to be the favored hypothesis, which may be tested in future studies.

a. Hypotheses explaining large-drop-dominant DSDs

In convective storms, large drops originate from melting of graupel and hailstones. But their source alone is not a sufficient explanation of their preferential location in certain parts of severe storms. The following subsections present explanations of how "big drop" regions can arise in the hook echoes of supercells.

1) Evaporation

Evaporation preferentially depletes the smaller drop sizes, which results in an increase in the DSD's median and thus ZDR (e.g., Li and Srivastava 2001; Kumjian and Ryzhkov 2010). Thus, an increase in ZDR and decrease in ZH is expected for DSDs that undergo evaporation. However, Kumjian and Ryzhkov (2010) show that the magnitude of changes in ZDR owing to evaporation alone (e.g., <0.5 dB, even in extreme cases) are eclipsed by those from other processes, including size sorting. In regions of large ZH (heavy rainfall), which characterizes much of the hook echo, evaporation becomes insignificant (e.g., Hu and Srivastava 1995). Small drops also are located very near the large drop regions, which is not expected if evaporation is dominant. Therefore, evaporation is unlikely to be the main contributor to the observed regions of large drops.

2) Size sorting

Size sorting can be invoked to explain the large Z_{DR} at the edge of the hook echo. Numerical simulations (e.g., Klemp et al. 1981; Klemp and Rotunno 1983; Wicker and Wilhelmson 1995, among others) and dual-Doppler analyses (e.g., Klemp et al. 1981; Brandes 1981, among others) indicate that the supercell updraft overlaps the inner edge of the hook (as shown by rainwater content in simulations, reflectivity factor in observations). Only the largest particles with the largest fall speeds can fall against the updraft on its periphery. Also, as the raindrops advect horizontally around the mesocyclone, the largest drops fall out first owing to their large fall speeds. This explains the Z_{DR} gradient parallel to the major axis of the hook echo sometimes observed at the upstream portion of the hook (where it connects to the main body of the storm). Therefore, size sorting provides a simple yet powerful explanation for the appearance of large-drop-dominant DSDs at the inflow edge and/or upstream portion of the hook echo. This high-Z_{DR} region often wraps around and connects with the Z_{DR} arc along the edge of the forward flank—also likely a result of size sorting, in this case by strong vertical wind shear (Kumjian and Ryzhkov 2008, 2009). The source of these large raindrops falling through or on the periphery of the updraft is melting of graupel and smaller hail that prevail in supercells.

Size sorting by centrifuging, as speculated in other studies (e.g., Van Den Broeke et al. 2008) can be ruled out. First, a simple scale analysis demonstrates that radial accelerations imparted on large drops by even strong mesocyclones are insufficient to displace the drops appreciable distances. Second, the small drops are located radially *farther* away from the center of circulation than the large drops. If centrifuging were occurring, the opposite would be true. Therefore, size sorting *by centrifuging* can be dismissed as an explanation for the large drop regions in hook echoes.

b. Hypotheses explaining small-drop-dominant DSDs

DSDs in heavy convective rain tend to be broad and superexponential in shape, with large concentrations of small drops as well as large drops (e.g., Brandes et al. 2003; Zhang et al. 2008; Cao and Zhang 2009). Nonetheless, these events do not produce the DSDs with

anomalously large concentrations of small drops and a lack of large drops seemingly characteristic of portions of supercell hook echoes. The following subsections present explanations of how anomalous concentrations of small drops can arise in supercell hook echoes.

1) Saturated conditions—no evaporation

Typically, large numbers of very small (<1 mm) drops are not observed at the surface, except perhaps in the cases of heavy drizzle or tropical rain. One major reason for this is that tiny drops often evaporate before reaching the ground, because of their very small fall speeds (<1 m s^{-1}) and preferential evaporation of smaller sizes (the rate of change in size D owing to evaporation $dD/dt \propto D^{-1}$). The slow descent of tiny drops provides ample time for evaporation. If supercell RFDs were saturated, no evaporation would take place to deplete the small drops before reaching the surface. However, this hypothesis seems very unlikely, as RFDs are rarely (if ever) saturated. In fact, the surface thermodynamic observations by Markowski et al. (2002) essentially rule out this possibility.

2) Enhanced breakup

Another possible explanation for the abundance of small drops is that the wind fields in and around supercell mesocyclones are such that collisional drop breakup is enhanced. Strong gradients of updraft and downdraft, strong rotation, and turbulence can alter substantially the three-dimensional velocities of particles, which affects the rates of collision and subsequent drop breakup (e.g., Khain and Pinsky 1995; Jonas 1996; Pinsky and Khain 1997; Sundaram and Collins 1997). The collision kernels for raindrops usually consider only vertical collisions (e.g., Low and List 1982; Brown 1986; Beard and Ochs 1995; Seifert et al. 2005). However, Khain and Pinsky (1995) and others show that deviant raindrop motion induced by strong shear and turbulence causes the drops to collide at angles off vertical, thereby enhancing the collision kernels. Wind-tunnel observations by Vohl et al. (1999) confirm these expectations, showing enhanced drop growth in turbulent flow (implying more collisions).

The resulting enhanced breakup of large drops would result in significant raindrop multiplication, especially for smaller sizes (e.g., Low and List 1982; Rosenfeld and Ulbrich 2003). If not balanced by coalescence, this multiplication would lead to an excess of smaller drops. In some mesoscale convective systems, the surging outflow gust front carries with it a small concentration of tiny drops, ahead of the precipitation line. It is possible that such fragments are produced by similar mechanisms described above in the strong outflow winds. However, radar and disdrometer observations (Schuur et al. 2001) show that supercell storms *still* contain very large drops, which suggests that breakup of these large drops is not a dominant process, or that they are continually replenished from the melting of small hail and graupel falling from aloft (e.g., Ryzhkov et al. 2009). Additionally, measurements of the Doppler spectrum width (σ_w) often reveal smaller values of σ_w in the RFD than in other parts of the storm (e.g., Yu et al. 2007), indicating that the flow is perhaps not very turbulent. Thus, though plausible for explaining the anomalously large concentration of small drops, it is not clear why enhanced break-up would lead to the observed spatial offset of small-drop and big-drop zones in the hook echo.

3) Dynamically induced downdrafts

If the DSDs in hook echoes are in fact intrinsic to supercells, one should look to microphysical and kinematic features that are typical of such storms. A major difference between supercells and other storm types is the large influence of pressure perturbations on the storm's evolution and dynamics. In particular, vertically-directed perturbation pressure gradient forces (VPPGFs) are known to play a role in the production or maintenance of the RFD (e.g., Lemon and Doswell 1979; Klemp and Rotunno 1983; Markowski 2002 and references therein). VPPGFs can arise from the interaction of strong environmental shear and the storm's updraft. Also, vertical gradients in vertical vorticity are associated with VPPGFs. A striking example of the latter is the "occlusion downdraft" (Klemp and Rotunno 1983), which forms when low-level vertical vorticity has amplified such that it exceeds the vertical vorticity aloft, resulting in a downward-directed VPPGF. The occlusion downdraft is a localized enhancement of the RFD, sometimes visually manifested as a "clear slot" that forms to the south or southeast of the center of circulation (e.g., Markowski 2002).

The RFD and occlusion downdraft are distinctive of supercell storms. In most other precipitation systems, downdraft development is

dominated by production of negative buoyancy via a combination of evaporation of raindrops, melting of hailstones, and precipitation loading. Evaporation acts preferentially on smaller raindrops; thus, appreciable quantities of the smallest raindrops rarely make it to the surface, as described above. However, if a downdraft is at least partly attributable to dynamic effects, the smaller drops may be transported downwards faster than they normally would fall. Indications that RFD air is partly comprised of parcels recycled from the boundary layer (Markowski et al. 2002), rather than mixing from dry air aloft, suggest that the RFD can remain relatively moist. Thus, in supercell RFDs the low lifting condensation levels (LCLs) and strong downdrafts can combine to rapidly transport smaller drops to lower levels than those at which they would be present otherwise.

But if a dynamically-induced downdraft is transporting smaller drops to the surface (negative vertical advection), larger drops also should be transported to the surface. Radar measurements, especially those at C band, are very sensitive to the presence of large drops. The observations provided in the previous section do not indicate the presence of an appreciable concentration of large drops in these suspected downdrafts, as the observed Z_{DR} is quite low in the rear portions of hook echoes, collocated with very high ρ_{hv}. This apparent discrepancy may be resolved by considering the source of tiny drops. The first possible source of small drops in the RFD is simply by transport from elsewhere in the storm. Wicker and Wilhelmson (1995) and others have found a substantial pathway along or through the forward-flank precipitation for air parcels which end up in the tornado. The tiny drops follow the airflow patterns very well because of their small terminal fall speeds, whereas the larger drops simply fall out. Thus, if such trajectories exist in real storms, small drops sorted from the portion of the Z_{DR} arc nearest to the inflow notch or from heavy precipitation in the core that are not scavenged by other falling particles may be transported cyclonically by the north side of the mesocyclone, where they enter the RFD and are transported to the ground. Precipitation trajectories based on dual-Doppler analyses or high-resolution numerical simulations may test this hypothesis.

Alternatively, it is more likely that there may be an additional source of small drops produced locally that end up in the RFD. If air from the moist boundary layer and/or the precipitation-cooled and moistened forward flank is lifted but remains at relatively low levels (beneath the environmental freezing level), then warm-rain processes initiated by such forced ascent of moist air would be an efficient process for producing appreciable quantities of smaller drops, but no very large drops (which arise from melting ice particles such as graupel and hail that fall from much farther aloft). Rather than being driven by buoyancy, moist air parcels can be drawn into the updraft dynamically or lifted along the rear-flank gust front. This rich supply of small drops is produced in close proximity to air flowing into the RFD, allowing the RFD to easily transport the drops downward. Preliminary modeling studies (e.g., Van Den Broeke and Straka 2010) indicate warm-rain generated, smaller drops are in fact present on the west side of the RFD and hook echo, at least in some of their idealized simulations.

In summary, we have presented several hypotheses explaining the exotic DSDs found in supercell hook echoes. By weighing the relative merits of each, we currently favor the explanations of size sorting (by the updraft) and dynamically-induced downdrafts (transporting small drops to the surface) for the large-drop and small-drop regions, respectively. Interestingly, the location of the small-drop regions of hook echoes corresponds to the expected locations of downdrafts (Fig. 7) in supercells: on the rear side of the hook echo, and on the southern side of the circulation (cf. Figs. 3-5). Also of note is that the high-Z_{DR} regions in observations correspond to the locations of expected updraft, where the simulated updraft overlays the rainwater content "hook."

4. Evolution of DSDs

Like all systems in nature, supercells evolve. Generally, however, the 4–5-min update times of WSR-88D radars are insufficient to capture the rapid evolution of supercells. To mitigate this problem, Kumjian et al. (2010) recently obtained polarimetric data using a rapid-scan strategy on a cyclic nontornadic supercell that moved through west-central Oklahoma on 1 June 2008. Full volume updates were achieved every 72 s, providing comparatively high temporal resolution. Oversampling in azimuth also allowed for increased spatial resolution. This unique dataset provides the opportunity to examine the evolution of the hook echo DSDs at finer temporal scales than previously available.

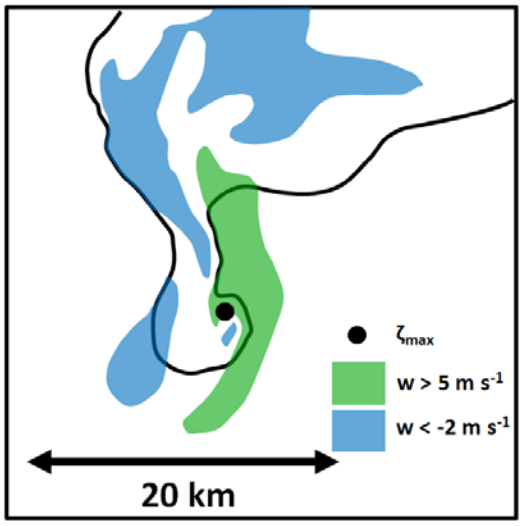

Figure 7: Vertical velocity field from a numerically simulated supercell at 1 km AGL. Updraft regions are shown in green, downdrafts in blue. The thick black line represents the rainwater mixing ratio 0.25 g kg^{-1} contour at 60 m AGL (a proxy for near-surface Z_H). The black dot locates the maximum vertical vorticity. Arrow indicates horizontal scale. Adapted from Fig. 3 in Wicker and Wilhelmson (1995).

For each Z_H value, the Cao et al. (2008) relation (Eq. 1) provides the "expected" Z_{DR} value typical of rainfall in Oklahoma. The "expected" Z_{DR} computed from Eq. (1) is compared to the observed Z_{DR} in the 1 June storm. Data from the 1 June supercell hook echo were subjected to a ρ_{hv} threshold of 0.97 to ensure the data points are mainly from rain.

For each time during the analysis period, the number of points with larger-than-expected Z_{DR} and smaller-than-expected Z_{DR} are counted. Natural DSD variability produces larger- and smaller-than-expected Z_{DR} values routinely; therefore, it is desirable to isolate the strongly skewed distributions by considering only severe departures from the Cao et al. relation. Thus, data points for which the observed Z_{DR} is more than 1 dB lower than the expected Z_{DR} (indicating drop size distributions strongly skewed towards smaller drops), and observed Z_{DR} values more than 1 dB higher than the expected Z_{DR} (indicating "big drop" distributions), are counted (Fig. 8). At the beginning of the analysis period, the number of large-drop points exceeds the number of small-drop points for the first two scans. Beginning at about 0336:41 UTC, there is a large increase in the small-drop points coincident with a lesser increase in the large-drop points. This increase occurs simultaneously with a surge in the RFD noted in single-Doppler velocity data (Kumjian et al. 2010). The ensuing occlusion of the mesocyclone is accompanied by a secondary maximum in small-drop points (between 0341:30 and 0343:55), and a decrease in the number of large-drop points, which diminishes to zero at 0343:55 UTC.

Low-level PPIs of Z_H reveal the hook echo in a characteristic "kinked" shape (Fig. 9) discussed in Beck et al. (2006), French et al. (2008) and Kumjian et al. (2010). The decrease in number of points with larger-than-expected Z_{DR}

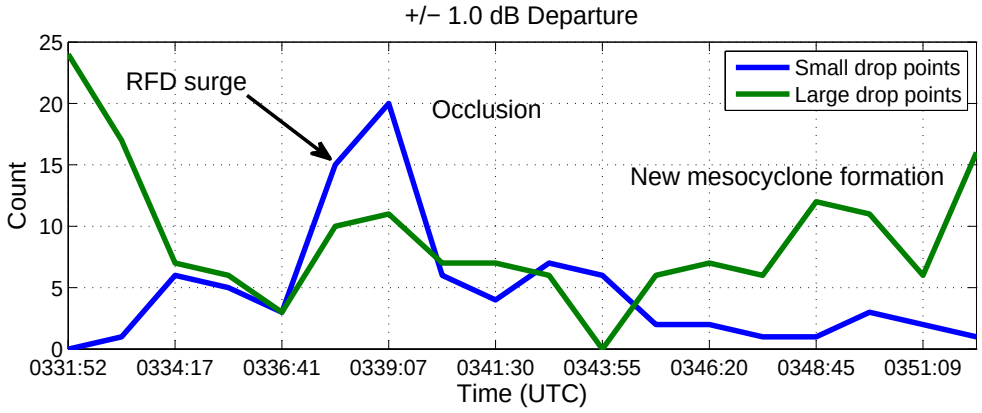

Figure 8: Time series of the number of hook echo data points with substantial (± 1 dB) observed departures from the "Cao et al." (expected) Z_{DR}. The blue line shows the "small drop points," or those characterized by Z_{DR} more than 1 dB lower than expected for its corresponding Z_H; the green line shows the "large drop points," or those characterized by Z_{DR} more than 1 dB higher than what is expected for its corresponding Z_H. Certain events in the storm's evolution (from Kumjian et al. 2010) are annotated.

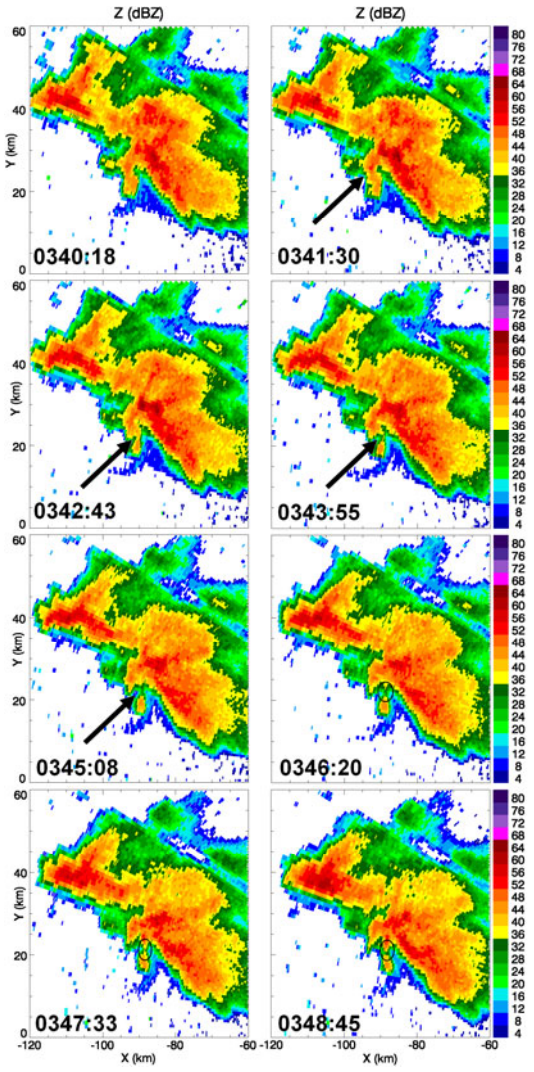

Figure 9: Low-level Z_H from 1 June 2008, at 0340:18–0348:45 UTC. Arrows indicate the "kink" in the hook echo. Circles represent areas of regeneration of Z_H (and very high Z_{DR}). *Click image to enlarge*.

may be the result of a weakening updraft, or a relative shift in location of the updraft and hook echo. At the apex of the kink, Z_H has decreased substantially (marked by the arrows in Fig. 9), indicating that precipitation pathways into this region are disrupted.

Following the occlusion of the low-level mesocyclone, a new circulation develops along the RFD gust front and begins to intensify. During this time (0346:20–0348:45 UTC), the hook echo Z_H values increase as it takes on a more cyclonically-curved shape (highlighted by ovals in Fig. 9), generally following the model of Beck et al. (2006). At the same time, Z_{DR} increases substantially near that portion of the hook echo connected to the main body of the storm. This increase in Z_{DR} associated with low-moderate Z_H is consistent with the increase in "large drop" points (Fig. 8). A re-intensification of the updraft as the new mesocyclone becomes established may enhance the Z_{DR} through sorting of the new drops falling into the hook as that pathway is reopened.

Though the trends are weak and shown for only one case, there is at least some preliminary suggestion that the hook echo precipitation characteristics are linked to the storm's behavior, especially the occlusion process. Picca and Ryzhkov (2010) and Picca et al. (2010) have demonstrated that increases in updraft strength, inferred from increases in the subfreezing volume of the Z_{DR} column, are associated with an intensification of the low-level precipitation core after a 10–20 min lag. Kumjian et al. (2010) and Palmer et al. (2011) found that the larger-scale polarimetric radar signatures in supercells follow repetitive patterns of evolution tied to the cyclic occlusion process. Thus, it is plausible that changes in the hook echo precipitation characteristics observed in the polarimetric radar measurements may be related to storm behavior, including occlusion of the mesocyclone, RFD surges, and changes in low-level updraft strength, albeit at shorter lags. This interesting possibility warrants future investigations with data of sufficient spatial and temporal resolution to capture the rapid, fine-scale changes in hook echoes. Such datasets may be available soon from the efforts of the VORTEX2 field campaign.

5. Summary of conclusions

This study offers a preliminary investigation into the characteristics of hook echo precipitation through the use of S- and C-band dual-polarization radar observations of tornadic and nontornadic supercells. Special cases of storms in close proximity to the radar or scanned with rapid sampling techniques afforded enhanced spatial and temporal resolution. A schematic conceptual model of the hook echo polarimetric features and vertical velocity fields is provided in Fig. 10. In this conceptual model, the back edge of the hook echo has DSDs dominated by small drops, often in anomalously high concentrations (green shaded region), generated by warm rain processes and transported to the ground in dynamically-forced downdrafts. Surges in the RFD or localized enhancements such as the occlusion downdraft (shaded in darker green)

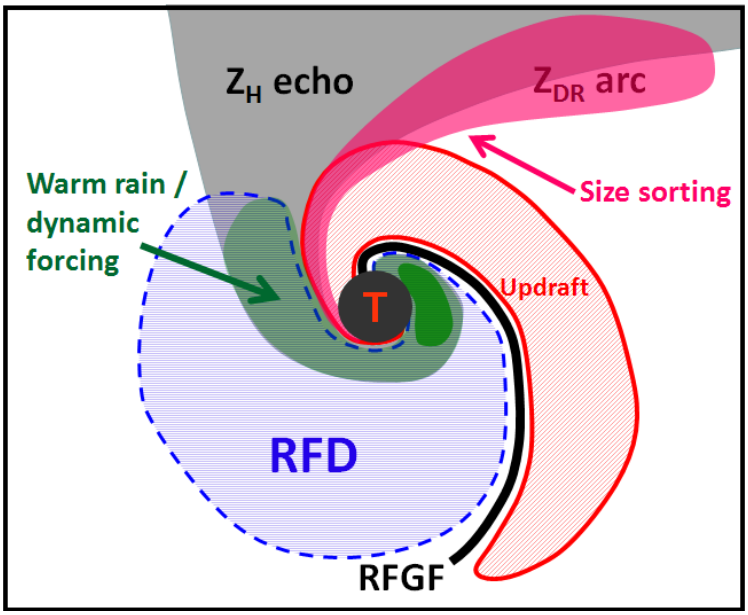

Figure 10: Conceptual model of the precipitation characteristics of supercell hook echoes overlaid with the locations of updraft (red), RFD (blue), and the primary rear-flank gust front (black line, RFGF). The region shaded in pink indicates large-drop zones with high Z_{DR} (including the Z_{DR} arc). The green shading represents regions of lower Z_{DR} and smaller drop sizes. The dark green region represents an enhancement in tiny drops transported by the occlusion downdraft. The location of the tornado is indicated by the black circle with a red "T".

could be characterized by an enhancement in small-drop concentrations. On the other hand, the inner (inflow) edge of the hook echo is a region of large drops (pink shading) falling out of the updraft above, sorted from the smaller drops (which are carried aloft).

The following key points are suggested:

1) Dual-polarization radar measurements provide evidence that drop size distributions (DSDs) in supercell hook echoes are exotic and atypical of rainfall in Oklahoma from other precipitating systems.

2) DSDs in hook echoes are spatially inhomogeneous, with large drop regions located on the inner/inflow edge and regions of very small drops located at the back of the hook that wrap around the southern and southeastern sides of the circulation.

3) Currently, the favored hypothesis explaining the presence of the large drop region is that of hydrometeor size sorting owing to the low-level updraft, such that only the largest drops are able to fall out of the updraft periphery. The small-drop region is hypothesized to originate in part from dynamically-induced downdrafts that transport the drops to the surface more rapidly than they otherwise would fall, preventing total depletion of the small drops by evaporation. Appreciable quantities of small drops could be produced locally at low levels by warm-rain processes resulting from forced ascent of moist boundary-layer air.

4) There is some evidence suggesting that the anomalously large concentrations of small drops together with regions of big drops in hook echoes are unique to supercell storms.

5) Weak trends in the DSD characteristics may be related to the occlusion process, including the rearward movement of the mesocyclone, RFD surge, and updraft weakening. However, the lack of statistical significance renders these relations uncertain and requires further investigation.

Future studies, especially those employing high-resolution dual-polarization radars or taking in situ measurements with disdrometers, may provide more definitive evidence for or against the conclusions above. The gradient of drop sizes across the hook echo is a feature that bulk

single-moment microphysics parameterizations are unable to reproduce. This shortcoming may have implications for attempts to deduce the thermodynamic characteristics of simulated RFDs, which are important for idealized studies of tornadogenesis. A better understanding of the links between supercell dynamics and the unique DSDs in hook echoes is warranted, especially if the microphysics is tied to storm evolution and behavior, as suggested in this study.

ACKNOWLEDGMENTS

The author thanks the NSSL/CIMMS staff who worked to ensure high-quality operation of KOUN. Funding for this study comes from NOAA/University of Oklahoma Cooperative Agreement NA17RJ1227 under the U.S. Dept. of Commerce. Some of the data presented were collected for research funded by NSF grant ATM-0532107. David Bodine (OU) is thanked for providing one of the OU-PRIME figures. OU-PRIME is maintained and operated by the Atmospheric Radar Research Center (ARRC) of the University of Oklahoma. Thoughtful discussions with Alex Schenkman (OU), Chad Shafer (Univ. of S. Alabama), Dan Dawson (NSSL), and Glen Romine (NCAR) contributed to the study. An early review of the manuscript by and discussions with Alexander Ryzhkov (CIMMS) are also appreciated. Helpful and thorough reviews by Johannes Dahl and Christopher Weiss have improved the clarity and presentation of the paper and are greatly appreciated. The author is also grateful for the expeditious and thorough editing by Roger Edwards and Amos Magliocco.

REFERENCES

Beard, K. V., and H. T. Ochs, 1995: Collisions between small precipitation drops. Part II: Formulas for coalescence, temporary coalescences, and satellites. *J. Atmos. Sci.*, **52**, 3977–3996.

Beck, J. R., J. L. Schroeder, and J. M. Wurman, 2006: High-resolution dual-Doppler analyses of the 29 May 2001 Kress, Texas, cyclic supercell. *Mon. Wea. Rev.*, **134**, 3125–3148.

Bodine, D., R. D. Palmer, M. R. Kumjian, and A. V. Ryzhkov, 2010: High-resolution OU-PRIME radar observations of a prolific tornado-producing supercell on 10 May 2010. Preprints, *25th Conf. on Severe Local Storms*, Denver, CO, Amer. Meteor. Soc., P8.4.

Brandes, E. A., 1981: Finestructure of the Del City-Edmond tornadic meso-circulation. *Mon. Wea. Rev.*, **109**, 635–647.

——, G. Zhang, and J. Vivekanandan, 2003: An evaluation of a drop distribution-based polarimetric radar rainfall estimator. *J. Appl. Meteor.*, **42**, 652–660.

Bringi, V. N., and V. Chandrasekar, 2001: *Polarimetric Doppler Weather Radar: Principles and Applications.* Cambridge University Press, 636 pp.

Brown, P. S., 1986: Parameterization of drop-spectrum evolution due to coalescence and breakup. *J. Atmos. Sci.*, **44**, 242–249.

Cao, Q., and G. Zhang, 2009: Errors in estimating raindrop size distribution parameters employing disdrometer and simulated raindrop spectra. *J. Appl. Meteor. Climatol.*, **48**, 406–425.

——, ——, E. Brandes, T. J. Schuur, A. V. Ryzhkov, and K. Ikeda, 2008: Analysis of video disdrometer and polarimetric radar data to characterize rain microphysics in Oklahoma. *J. Appl. Meteor. Climatol.*, **47**, 2238–2255.

Dawson, D. T., and G. S. Romine, 2010: A preliminary survey of DSD measurements collected during VORTEX-2. Preprints, *25th Conf. on Severe Local Storms*, Denver, CO, Amer. Meteor. Soc., 8A.4.

Doviak, R. J., and D. S. Zrnić, 1993: *Doppler Radar and Weather Observations*. Academic Press, 562 pp.

Dowell, D. C., C. R. Alexander, J. M. Wurman, and L.J. Wicker, 2005: Centrifuging of hydrometeors and debris in tornadoes: radar-reflectivity patterns and wind-measurement errors. *Mon. Wea. Rev.*, **133**, 1501–1524.

French, M. M., H. B. Bluestein, D. C. Dowell, L. J. Wicker, M. R. Kramar, and A. L. Pazmany, 2008: High-resolution, mobile Doppler radar observations of cyclic mesocyclogenesis in a supercell. *Mon. Wea. Rev.*, **136**, 4997–5016.

Grzych, M. L., B. D. Lee, and C. A. Finley, 2007: Thermodynamic analysis of supercell rear-flank downdrafts from project ANSWERS. *Mon. Wea. Rev.*, **135**, 240–246.

Herzegh, P. H., and A. R. Jameson, 1992: Observing precipitation through dual-polarization radar measurements. *Bull. Amer. Meteor. Soc.*, **73**, 1365–1374.

Hirth, B. D., J. L. Schroeder, and C. C. Weiss, 2008: Surface analysis of the rear-flank downdraft outflow in two tornadic supercells. *Mon. Wea. Rev.*, **136**, 2344–2363.

Hu, Z., and R. C. Srivastava, 1995: Evolution of raindrop size distribution by coalescence, breakup, and evaporation: Theory and observations. *J. Atmos. Sci.*, **52**, 1761–1783.

Jonas, P. R., 1996: Turbulence and cloud microphysics. *Atmos. Res.*, **40**, 283–306.

Khain, A., and M. Pinsky, 1995: Drop inertia and its contribution to turbulent coalescence in convective clouds. Part I: Drop fall in the flow with random horizontal velocity. *J. Atmos. Sci*., **52**, 196–206.

Klemp, J. B., and R. Rotunno, 1983: A study of the tornadic region within a supercell thunderstorm. *J. Atmos. Sci.*, **40**, 359–377.

——, R. B. Wilhelmson, and P. S. Ray, 1981: Observed and numerically simulated structure of a mature supercell thunderstorm. *J. Atmos. Sci.*, **38**, 1558–1580.

Kumjian, M. R., and A. V. Ryzhkov, 2008: Polarimetric signatures in supercell thunderstorms. *J. Appl. Meteor. Climatol.*, **47**, 1940–1961.

——, and ——, 2009: Storm-relative helicity revealed from polarimetric radar observations. *J. Atmos. Sci.*, **66**, 667–685.

——, and ——, 2010: The impact of evaporation on polarimetric characteristics of rain: Theoretical model and practical implications. *J. Appl. Meteor. Climatol.*, **49**, 1247–1267.

——, ——, V. Melnikov, and T. J. Schuur, 2010: Rapid-scan super-resolution observations of a cyclic supercell using a dual-polarization WSR-88D. *Mon. Wea. Rev.*,**138**, 3762–3786.

Lemon, L. R., and C. A. Doswell III, 1979: Severe thunderstorm evolution and mesocyclone structure as related to tornadogenesis. *Mon. Wea. Rev.*, **107**, 1184–1197.

Li, X., and R. C. Srivastava, 2001: An analytical solution for raindrop evaporation and its application to radar rainfall measurements. *J. Appl. Meteor.*, **40**, 1607–1616.

Low, T. B., and R. List, 1982: Collision, coalescence, and breakup of raindrops. Part II: Parameterization of fragment size distributions. *J. Atmos. Sci.*, **39**, 1607–1618.

Markowski, P. M., 2002: Hook echoes and rear-flank downdrafts: A review. *Mon. Wea. Rev.*, **130**, 852–876.

——, J. M. Straka, and E. N. Rasmussen, 2002: Direct surface thermodynamic observations within the rear-flank downdrafts of nontornadic and tornadic supercells. *Mon. Wea. Rev.*, **130**, 1692–1721.

——, ——, and ——, 2003: Tornadogenesis resulting from the transport of circulation by a downdraft: Idealized numerical simulations. *J. Atmos. Sci.*, **60**, 795–823.

Palmer, R. D., D. Bodine, M. R. Kumjian, B. Cheong, G. Zhang, Q. Cao, H. B. Bluestein, A. Ryzhkov, T.-Y. Yu, and Y. Wang, 2011: Observations of the 10 May 2010 tornado outbreak with OU-PRIME: Potential for new science with high-resolution polarimetric radar. *Bull. Amer. Meteor. Soc.,* **92**, 871–891**.**

Picca, J. C., and A. V. Ryzhkov, 2010: Polarimetric signatures of melting hail at S and C bands: Detection and short-term forecast. Preprints, *26th Conf. on Interactive Information and Processing Systems*, Atlanta, GA, Amer. Meteor. Soc., 10B.4.

——, M. R. Kumjian, and A. V. Ryzhkov, 2010: Z_{DR} columns as a predictive tool for hail growth and storm evolution. Preprints, *25th Conf. on Severe Local Storms*, Denver, CO, Amer. Meteor. Soc., 11.3.

Pinsky, M., and A. P. Khain, 1997: Formation of inhomogeneity in drop concentration induced by drop inertia and their contribution to the drop spectrum broadening. *Quart. J. Roy. Meteor. Soc.*, **123,** 165–186.

Pruppacher, H. R., and K. V. Beard, 1970: A wind tunnel investigation of the internal circulation and shape of water drops falling at terminal velocity in air. *Quart. J. Roy. Meteor. Soc.*, **96**, 247–256.

Romine, G. S., D. W. Burgess, and R. B. Wilhelmson, 2008: A dual-polarization radar-based assessment of the 8 May 2003 Oklahoma City area tornadic supercell. *Mon. Wea. Rev.*, **136**, 2849–2870.

Rosenfeld, D., and C. W. Ulbrich, 2003: Cloud microphysical properties, processes, and rainfall estimation opportunities. *Radar and Atmospheric Science: A Collection of Essays in Honor of David Atlas*, *Meteor. Monogr.*, No. 52, Amer. Meteor. Soc., 237–258.

Ryzhkov, A. V., T. J. Schuur, D. W. Burgess, P. L. Heinselman, S. E. Giangrande, and D. S Zrnić, 2005a: The Joint Polarization Experiment: Polarimetric rainfall measurements and hydrometeor classification. *Bull. Amer. Meteor. Soc.*, **86**, 809–824.

——, ——, ——, and D. S. Zrnić, 2005b: Polarimetric tornado detection. *J. Appl. Meteor.*, **44**, 557–570.

——, S. Ganson, A. Khain, M. Pinsky, and A. Pokrovsky, 2009: Polarimetric characteristics of melting hail at S and C bands. Preprints, *34th Conf. on Radar Meteorology,* Williamsburg, VA, Amer. Meteor. Soc., 4A.6.

Schuur, T. J., A. V. Ryzhkov, D. S. Zrnić, and M. Schönhuber, 2001: Drop size distributions measured by a 2D video disdrometer: Comparison with dual-polarization radar data. *J. Appl. Meteor.*, **40**, 1019–1034.

Seifert, A., A. Khain, U. Blahak, and K. D. Beheng, 2005: Possible effects of collisional breakup on mixed-phase deep convection simulated by a spectral (bin) cloud model. *J. Atmos. Sci.*, **62**, 1917–1931.

Straka, J. S., D. S. Zrnić, and A. V. Ryzhkov, 2000: Bulk hydrometeor classification and quantification using polarimetric radar data: Synthesis of relations. *J. Appl. Meteor.*, **39**, 1341–1372.

Sundaram, S., and L. R. Collins, 1997: Collision statistics in an isotropic particle-laden turbulent suspension. Part 1: Direct numerical simulations. *J. Fluid Mech.*, **335**, 75–109.

Van Den Broeke, M. S., and J. M. Straka, 2010: Mesocyclone and RFD evolution in simulated supercell storms with varying wind profiles. Preprints, *25th Conf. on Severe Local Storms*, Amer. Meteor. Soc., Denver, CO, 8A.6.

——, ——, and E. N. Rasmussen, 2008: Polarimetric radar observations at low levels during tornado life cycles in a small sample of classic Southern Plains supercells. *J. Appl. Meteor. Climatol*, **47**, 1232–1247.

Vohl, O., S. K. Mitra, S. C. Wurzler, and H. R. Pruppacher, 1999: A wind tunnel study of the effects of turbulence on the growth of cloud droplets by collision and coalescence. *J. Atmos. Sci.*, **56**, 4088–4099.

Wicker, L. J., and R. B. Wilhelmson, 1995: Simulation and analysis of tornado development and decay within a three-dimensional supercell storm. *J. Atmos. Sci.*, **52**, 2675–2703.

Wurman, J., and S. Gill, 2000: Finescale radar observations of the Dimmitt, Texas (2 June 1995), tornado. *Mon. Wea. Rev.*, **128**, 2135–2164.

Yu, T.-Y., Y. Wang, A. Shapiro, M. B. Yeary, D. S. Zrnić, and R.J. Doviak, 2007: Characterization of tornado spectral signatures using higher-order spectra. *J. Atmos. Oceanic Technol.*, **24**, 1997–2013.

Zhang, G., M. Xue, Q. Cao, and D. Dawson, 2008: Diagnosing the intercept parameter for exponential raindrop size distribution based on video disdrometer observations: Model development. *J. Appl. Meteor. Climatol.*, **47**, 2983–2992.

Zrnić, D. S., and A. V. Ryzhkov, 1999: Polarimetry for weather surveillance radars. *Bull. Amer. Meteor. Soc.*, **80**, 389–346.

REVIEWER COMMENTS

[Authors' responses in *blue italics.*]

REVIEWER A (Johannes Dahl):

Initial Review:

Recommendation: Acceptable with minor revisions.

Overview: The study convincingly identifies unusual drop-size distributions (DSDs) in the hook echoes of supercells. Several hypotheses to explain these DSDs are discussed, and the temporal evolution of the DSD during a hook-echo replacement cycle is presented for one case.

Although the explanations of the observations are rather speculative, they reflect how little we know about the microphysical processes in supercells. The hypotheses provided are the first step towards a more solid understanding that hopefully will be developed in future studies. In my opinion, the paper contains important and new observations and is well suited for publication in EJSSM. I have a couple of small/technical comments but only two substantive ones.

Substantive Comments:

i. After Section 2b, a brief summary of the cases that are considered in the subsequent paragraphs should be presented (this could be as short as a table, including the dates/times, which radar was used to obtain the data in each case, etc.). As later in the text one of the 10 May 2010 storms is referred to as the "Norman supercell", perhaps introduce this label in the text (or table). Also, I thought it was somewhat confusing to have altogether six cases, but only pieces of different observations of each case are considered (e.g., although polarimetric data from the 1 June 2008 case seem to exist, PPI displays of these data are not shown). Adding some information about these cases would help clarify section 2c.

Good points. To provide the reader with more information about these cases, a table has been added with the dates, times and radar used to collect the data of each storm. The two from 10 May 2010 collected with OU-PRIME have names "Moore" and "Norman" in the table, and a call to Table 1 has been added to the text to alleviate any confusion about that storm.

A PPI image of low-level Z_H from each of the four cases shown in the old Fig. 1 (scatterplots) has also been added to offer some context of what the storms look like. This is the new Fig. 1. Because low-level PPIs are already shown for the two OU-PRIME cases, they were not repeated in this new figure. In addition, some text has been added to this section (as well as the previous section on methods) to explain more clearly that the four KOUN cases (shown now in Fig. 1 and listed in Table 1) are used in the scattergram analysis (now Fig. 2), and why the C-band cases are not used (the ρ_{hv} threshold cannot be applied to isolate rain from rain/hail mixtures).

Concerning the 1 June 2008 case (which is used extensively in the DSD evolution section), there is already a figure with Z_H every ~1 min (now Fig. 9). Plenty of polarimetric data from this case are shown in Kumjian et al. (2010; Monthly Weather Review), but could also be shown here if you think it will add to the paper.

The text describing the "Norman supercell" and its second tornado has been deleted on recommendation from another reviewer.

ii. Regarding the discussion of the temporal evolution of the scatter diagrams (Fig. 7): The overall decrease of larger-than-expected Z_{DR} before 0343:55 UTC is rather clearly seen in the figures (except perhaps at 0341:30 UTC, but there does seem to be an overall decreasing trend). However, I have difficulties seeing the described increase of Z_{DR} below the one-to-one line. For instance, just by looking at the plots it is not at all obvious that at 0346:20 UTC there are more points below the line than at 0342:43 UTC (or at 0341:30

UTC). To convince the reader that the described trend exists, this increase needs to be quantified—e.g., by using a simple plot of "number of points below the line" as a function of time.

This is a great suggestion. I think the presentation is much *clearer with the simple "count" of points above or below the line. To accentuate those points that are substantial departures from what is expected in Oklahoma rain, I have selected the threshold of ±1 dB in Z_{DR}. Thus, only points that are more than 1 dB higher than expected (or 1 dB lower than expected) for a given Z_H are counted. This allows us to look past the slight/natural variations in Z_{DR} to the more unusual/severe departures. The trends are rather similar using ±0.75 dB or ±1.25 dB as well, so I stuck with 1.0 dB as a nice round number.*

In doing so, I think it illuminates even more the changes in hook echo DSD characteristics associated with the storm's evolution, which have been annotated on the figure. For example, the large jump in number of small-drop points coincident with the RFD surge is striking. The image has been replaced and the text modified to account for the new figure (and new information that can be gleaned from it).

[Minor comments omitted...]

Second review:

Recommendation: Accept.

General Comments: I have no more comments that would necessitate another review cycle. I think the manuscript is acceptable for publication now.

REVIEWER B (Christopher C. Weiss):

Initial Review:

Reviewer recommendation: Accept with minor revisions.

Synopsis: This paper presents some unique dual-polarization radar measurements of hook echoes within supercell thunderstorms. These measurements cover two different platforms/frequencies, including OU-PRIME (C-band) and the KOUN polarimetric radar (S-band). The primary finding of the paper is a repeatable distribution of certain polarimetric variables across the expanse of the hook, in tandem identifying a large drop population for inside trajectories and a wealth of small drops for the remaining body of the hook. These populations are shown to depart from the Z_{DR}/Z_H relationship for typical Oklahoma rainfalls (exclusive of this supercell mode), suggesting that there is an anomalously large number of small drops within this latter region, the implications of which could be substantial for the potential of increased evaporation and aggressive cold pool production within supercells.

Overall, the paper is well-written and was an enjoyable read. Have some suggestions for improvements and some requests for clarifications on a few items below.

Substantive Comments:

1) [Introduction]: The findings of Markowski et al. (2002) are accurately stated, that weaker deficits in equivalent and potential temperature within the RFD are more typical of tornadic storms. It is worth mentioning that exceptions exist where tornadoes exist within more negatively buoyant downdraft regimes, such as that discussed by Hirth et al. (2008) and Romine et al. (2008), among others.

Good point. I have added a bit of text describing these exceptions and the references. It is important to note (and has been in the revised text) that while thermodynamic characteristics of the RFDs are seemingly important for tornadogenesis, they don't tell the whole story. This is something that the original Markowski et al. (2002) paper emphasizes in its conclusions, but perhaps has not been as widely recognized in the field.

2) Figure 1: The wealth of data points below the Cao et al. (2008) curve within the hook region is certainly noteworthy, and germane to the arguments put forth in the paper. Also intriguing to me is that the great majority of the rest of the (black) data points sit above the Cao et al (2008) curve. I may have missed it, but I didn't see mention of this fact in the text. What does this bias indicate? Perhaps that, across the spectrum of reflectivity, we tend to have a small number of large drops, rather than a larger number of smaller drops?

You are correct, especially for the lower Z_H values. The initial description in the text (end of the paragraph in which Fig. 1 is introduced) probably was too brief and only specifically mentions the low-Z_H points. The Cao et al. (2008) curve considers all types of precipitation, including a lot of weaker convection and stratiform events in which large drops (>6 mm) are comparatively rare. In strong convective storms, especially supercells, hail production can be quite prolific. Melting of the smaller hailstones contributes to an enhancement in the "big drop" end of the spectrum, which tends to push Z_{DR} upwards for all Z_H values. For the larger Z_H values, it is difficult to say if there is actually a lack of small drops when Z_{DR} is high (because the big drops overwhelm the signal). So, I hesitate to say "…rather than a larger number of small drops." In fact, convective DSDs tend to be superexponential in shape (i.e., negative shape parameter) which implies a large number of small drops in addition to a relatively large number of big drops.

A discussion of this issue has been added after the discussion of hook echo points in the text.

3) The [text] discussion of the polarimetric characteristics of the second tornado at the periphery of Fig. 4 is rather distracting in its present form, and somewhat out of place with the overall topic of hook echo characteristics. The explanation of the polarimetric properties of this second tornado comes across rather speculative, perhaps since there is not a lot of context. Would recommend that the author remove that portion of the discussion or devote a separate section to the topic with more development (e.g., evolution of pol parameters in time to support the differential sedimentation hypothesis along the RFGF).

Agreed. It was included because it was an interesting observation. However, there is not much context available because it was not sampled adequately prior to this scan (cut off by the sector). Plus, it is described a bit more in Palmer et al. (2011, BAMS). So, the text has been removed.

4) Regarding the size-sorting hypothesis for the generation of a large-drop dominant RFD, it is stated that large raindrops advected around the mesocyclone fall out first owing to large terminal fall speeds. Certainly agree on that, but how does that process explain the gradients in polarimetric properties *normal* to the trajectory (the inside/outside of the hook as in Fig. 4). If this process was dominant, wouldn't the signal be to have high Z_{DR} in the upstream portion of the hook, with low Z_{DR} downstream (i.e., gradients *parallel* to the trajectory)?

This part was included more to explain the instances where the high Z_{DR} is located at the upstream part of the hook (near where it connects to the main body of the storm; e.g., you can see some of this in Fig. 3). I do not think it is dominant, especially compared to the updraft sorting, which better explains the gradient normal to the trajectories entering the hook. However, in the instances where it appears as if the Z_{DR} arc wraps all the way into the hook, it may explain the gradients that are parallel to the hook major axis.

I've tried to clarify this in the text. Also, to make sure it does not come across as the dominant mechanism, I've used "sometimes" to describe the less frequent appearance of this sort of Z_{DR} gradient.

5) Playing devil's advocate here: Could an alternate hypothesis for the lateral gradients in Z_{DR} be simply attributable to the span of trajectories entering the hook region? In other words, trajectories forming the inside of the hook have a history of moving through regions with high Z_{DR} (e.g., large drops), while the areas upstream of the rest of the hook move through regions with smaller drops. Could the hook, then, just be a contraction of the span of Z_{DR} across the forward flank region of the supercell? I am not saying I believe this argument, but how would you respond?

I've considered this option. However, the main problem is that air parcel trajectories are not the same as precipitation particle trajectories, owing to precipitation particle inertia (i.e., raindrops have their own negative vertical velocity, whereas air parcels must follow the wind).

Consider for example the Z_{DR} arc region as a source of the big drops that wind up in the hook echo (as the devil's advocate has suggested). The Z_{DR} arc (region of high Z_{DR} along the southern edge of the forward flank precipitation echo) is observed at low levels, generally <2 km AGL. So, we can consider what type of horizontal flow is necessary to advect these drops from the FFD region to the hook echo. For the cases shown in this paper, a typical horizontal distance is roughly 10 to 20 km from Z_{DR} arc to hook echo. Large drops fall at about 8–10 m s^{-1}, depending on what velocity relation you choose (this is at the surface—they fall faster aloft). A simple scaling analysis with the "best" possible choices: minimum horizontal distance to travel (10 km), maximum distance to fall (2 km), slowest fall speed (8 m s^{-1}), results in a horizontal drop speed of 40 m s^{-1}. This is pretty intense, but not out of the question. However, at this speed, the smaller drops (1–2 m s^{-1} fall speeds in the absence of a downdraft) would have to come from a very, very large distance. With a sufficiently strong downdraft that increases the small drop negative vertical velocity, one could argue this may be a possible scenario. For larger horizontal distances, however, unreasonably large horizontal winds are required to advect drops from the forward flank to the hook echo.

Thus, while possible on the smaller scale (e.g., maybe out of the core and into the upstream portion of the hook echo), I do not think we can consider the hook echo Z_{DR} gradient to simply be a contraction of that which is observed in the forward flank.

[Minor comments omitted...]

Second review:

Recommendation: Accept with minor revision.

[Minor comments omitted...]